Dissociative Adsorption of Methylsilane on the Si(100)-2 × 1 Surface

Yong-Quan Qu, Jing Li, and Ke-Li Han*

Center for Computational Chemistry, Dalian Institute of Chemical Physics, Chinese Academy of Sciences, Dalian, People's Republic of China 116023

Received: November 26, 2003; In Final Form: June 24, 2004

Density functional theory calculations have been used to investigate the mechanisms of dissociative adsorption of methylsilane (CH_3SiH_3) on the Si(100)-2 × 1 surface. Three different reaction pathways via Si−H, C−H, and Si−C dissociation are used to describe the formation of $-SiH_2CH_3$, $-CH_2SiH_3$, $-CH_3$, $-SiH_3$, and −H fragments adsorbed on the dimer dangling bonds. The geometry, energetics, and vibration properties of the critical points along the potential energy surface using the Si_9H_{12} one-dimer and $Si_{15}H_{16}$ two-dimer cluster models are investigated. Our results indicate that the product of Si−H dissociation is the dominating dissociative product. The results also show that methylsilane is a good candidate for the growth of SiC films.

1. Introduction

Silicon carbide is a promising class of material used for high-temperature and high-power electronic devices because of its wide band gap and chemical and thermal stability. Thin film growth of SiC materials at semiconductor surfaces has become one of the most important areas for applications ranging from microelectronic devices to nanotechnology. Much effort has been made on the growth of crystalline SiC. Usually SiC film is grown on Si single crystals by chemical vapor deposition (CVD) using Si- and C-containing source gases, such as silanes (SiH_4, Si_2H_6) and alkanes (C_3H_8, C_2H_2, C_2H_4).[1,2] The Si:C ratio of SiC films is adjusted by changing the gas flow ratio of silane to hydrocarbons. This method, however, requires the independent flow control of each source gas and rather high temperature, which likely induces high tensile stress and crystalline lattice defects in SiC films. To relieve the above bottlenecks, the use of a "single" precursor containing both Si and C atoms has many advantages, such as a simplified CVD process, more efficient deposition, a higher degree of safety in operation, and a lower substrate temperature. Perhaps the most potential advantage is that the Si:C ratio of deposited SiC films may be varied significantly by changing the ratio of Si:C in the precursor and preserving Si−C bonds in the film growth and subsequently the quality of the film.

Recently, it has been revealed that β-silicon carbide film can be synthesized by using single precursors, such as methylsilane,[3−11] dimethylethylsilane,[12] hexamethyldisilane,[13,14] silacyclobutane,[15] disilabutane,[16] and dimethylisopropylsilane.[17] For substituted silanes containing a functional group other than the $-SiH_3$ group, the reactivity of molecules at the semiconductor surfaces will change. The current knowledge of the adsorption and reaction of these substituted silanes on silicon surfaces is rather limited.

Among these substituted silane molecule precursors, methylsilane has recently received much attention as a promising candidate for low-temperature SiC film growth. Xu et al.[5] used temperature programmed desorption experiments to investigate the adsorption and dissociation of methylsilane on the Si(100)-2 × 1 surface. The saturation coverage of the methylsilane on the Si(100)-2 × 1 surface at 300 K is about half that at 90 K. This is explained by assuming that more active surface sites are blocked and inhibit the further adsorption at high temperature due to dissociation of methylsilane and bonding of the resulting fragments to Si(100) surface dangling bonds. The steric arguments, based on the van der Waals radii of the fragments involved, suggest that the Si−C bond breakage among different possible dissociative chemisorption processes is the most likely to occur, with the production of SiH_3 and CH_3 groups attached to the Si(100)-2 × 1 surface dimers. Shinohara et al.[9,10] employed infrared absorption spectroscopy in the Si−H stretching vibration region to investigate carbon incorporation during CVD of SiC on the Si(100)-2 × 1 surface by methylsilane in the temperature range 300−400 °C. Their results suggest that breaking of the Si−H bonds of methylsilane molecules is more favorable than dissociation of the Si−C bond.

Because all the bonds of the methylsilane molecule are saturated, adsorption on the Si(100)-2 × 1 surface is expected to occur either after molecular dissociation or through a transition state. Xu et al.[5] postulated that there exists a transition state characterized by a pentacoordinated silicon atom. According to them, the dissociation of the methylsilane molecule may proceed at 300 K through a mechanism similar to the nucleophilic substitution (S_N2) reaction. In their opinion, the nucleophilic reagent (the "up" silicon atom of the surface dimer) attacks the silicon atom opposite the leaving group (CH_3 group) in the methylsilane molecule, resulting in the formation of the pentacoordinated transition state. However, no evidence has proved the existence of the pentacoordinated transition state.

Since it is important to understand the properties of the interface at the atomic level, we perform our calculations using density functional theory (DFT) to clarify the surface reactions of methylsilane on the Si(100)-2 × 1 surface during the initial step of adsorption. The possible dissociations through Si−H, C−H, and Si−C bond breaking in methylsilane molecule are schematically represented in Figure 1. The theoretical details are described in section 2. The calculated results are presented in section 3 as is a discussion of the selectivity, and competition of different dissociative pathways compared with experiments is illustrated in section 3. The stability of dissociated products is also presented in section 3.

* Corresponding author. E-mail: klhan@dicp.ac.cn.

10.1021/jp0376018 CCC: $27.50
Published on Web 08/31/2004

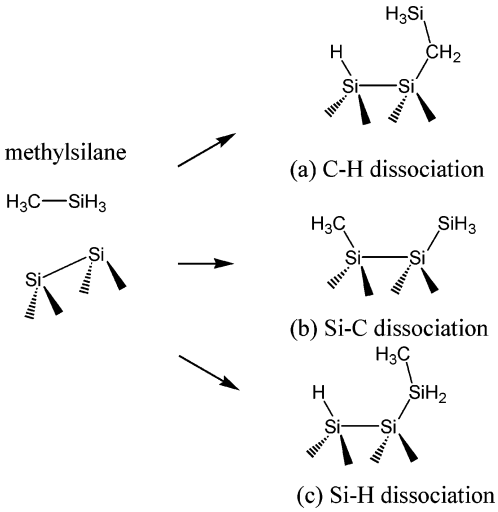

Figure 1. Possible surface reaction pathways of methylsilane on the Si(100)-2 × 1 surface during the initial step of adsorption: (a) C−H dissociation; (b) Si−C dissociation; (c) Si−H dissociation.

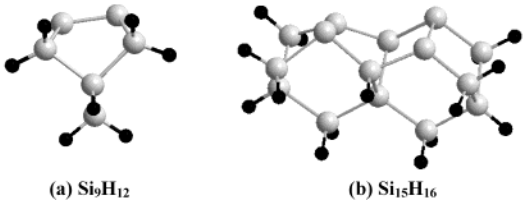

Figure 2. Cluster model for the clean Si(100)-2 × 1 surface: (a) Si_9H_{12} one-dimer cluster; (b) $Si_{15}H_{16}$ two-dimer cluster.

2. Theoretical Details

Si_9H_{12} one-dimer and $Si_{15}H_{16}$ two-dimer clusters are used to model the surface reactions of methylsilane on the clean Si(100)-2 × 1 surface. The one-dimer cluster consists of two surface silicon atoms representing the surface dimer and seven silicon atoms representing three layers of subsurface bulk atoms as described in many theoretical studies.[18−36] The two-dimer cluster contains four surface silicon atoms and eleven subsurface silicon atoms as shown in Figure 2b. The dangling bonds of the subsurface silicon atoms are terminated by hydrogen atoms in order to preserve the sp^3 bonding character of the subsurface silicon atoms and avoid the nonphysical effects that stem from subsurface dangling bonds. However, the terminating hydrogen may create a different chemical environment from the actual Si(100)-2 × 1 surface at the cluster boundary. Widjaja and Musgrave[37] have used cluster models of various sizes to verify that the error is insignificant.

In this work, we use the B3LYP[38−40] three-parameter gradient corrected hybrid density functional theory (DFT[41,42]) method for all electronic structures with the Gaussian 98[43] software package. B3LYP has been used extensively to calculate organic reactions on the Si(100)-2 × 1 surface[18−36] with the cluster approximation. These results are generally in good agreement with experiments. In the theoretical investigation on chlorosilanes on the Si(100)-2 × 1 surface,[28] Hall et al. have gauged the accuracy of B3LYP by comparing the results of B3LYP and QCISD. Therefore, it is expected that B3LYP is reasonable for the present system due to the similarity of methylsilane and chlorosilanes. The geometries of all minima and transition states in the potential energy surfaces in this work were calculated at the B3LYP/6-31G(d) level of theory without applications of geometry constraints or symmetry restrictions on the clusters. All calculated transition states on the potential energy surfaces were verified by frequency calculations to have one and only one imaginary frequency and followed by intrinsic reaction coordinate (IRC) calculations. Single point energy calculations were performed on the optimized structures at the B3LYP level of theory with a mixed basis set scheme in order to enhance the accuracy of calculations and minimize computational cost. The 6-311++G(2df,pd) basis set was used to describe the surface dimer silicon atoms and the methylsilane molecule, and the 6-31G(d) basis set was used to describe the subsurface atoms and the terminating hydrogen atoms. The energies reported have been corrected by zero-point energy under the same level of theory.

TABLE 1: Geometric Parameters of the Free Methylsilane Molecule, Compared with Experimental Values and Previous Theoretical Results

	our calcn	expt[44,45]	ref 46	ref 47
C−H (Å)	1.092	1.096	1.098	1.085
Si−H (Å)	1.483	1.483	1.486	1.476
C−Si (Å)	1.880	1.869	1.884	1.880
HCSi (deg)	110.8	110.9	110.8	111.2
HSiC (deg)	110.6	110.5	110.9	110.7

3. Results and Discussion

A. The Structure of Methylsilane. At first, we calculated the structural parameters of the free methylsilane molecule (Table 1) under the B3LYP/6-311++G(2df, pd) level of theory and found good agreement with the experimental results and previous theoretical calculations. Charge distribution of the molecule ($q_{Si} = +0.63$, $q_{H-Si} = -0.17$, $q_C = -0.32$, and $q_{H-C} = +0.07$) was computed with the ChelpG[47] method and performed at the same theory level in Gaussian 98.

B. Dissociative Pathways of Methylsilane at Si_9H_{12} One-Dimer Cluster. A wealth of experimental evidences and DFT calculations reveals that the Si(100)-2 × 1 surface dimer is buckled or tilted. This tilting gives the dimer a zwitterion-like character in which the "down" silicon atom is slightly positive relative to the "up" silicon atom. Many earlier theoretical studies[18−36] have shown that the dimer tilting is an essential feature of the transition states for the adsorption of organic molecules on the Si(100)-2 × 1 surface. In the present case, the silicon atom of methylsilane working as an electrophilic reagent and the carbon atom of methylsilane functioning as a nucleophilic reagent can react with surface dimers.

The calculated relative energies and geometric structures for the C−H, Si−H, and Si−C bond dissociation along the reaction pathways are shown in Figure 3 and Figure 4, respectively. For C−H dissociation, the calculations indicate that methylsilane undergoes a direct dissociation on the Si(100)-2 × 1 surface

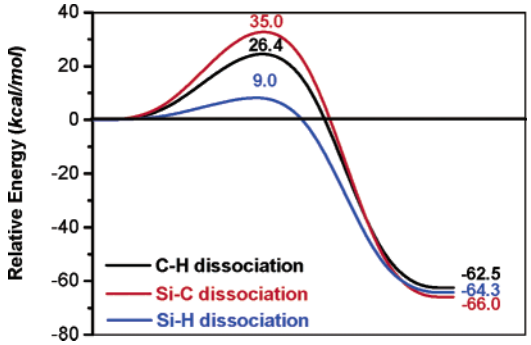

Figure 3. Reaction pathways for C−H, Si−C, and Si−H dissociation involving Si_9H_{12} one-dimer cluster. The black curve represents the C−H dissociation; the red curve represents the Si−C dissociation; the blue curve represents the Si−H dissociation.

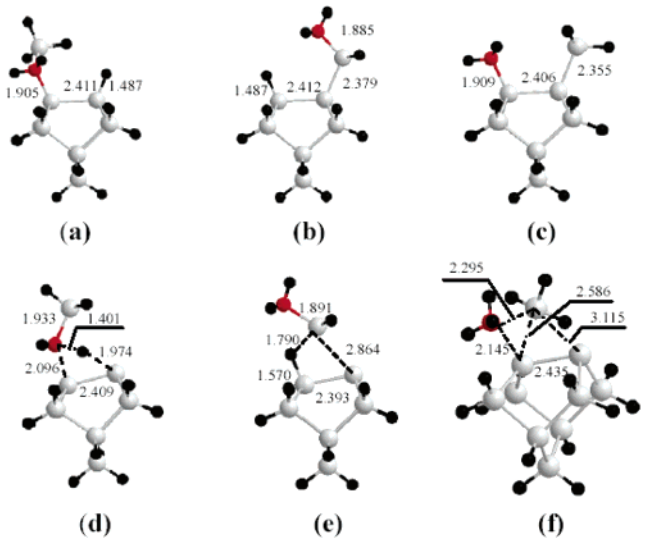

Figure 4. Calculated geometry structures of surface products and transition states along the surface reaction pathways at Si_9H_{12} one-dimer cluster: (a) the product of C−H dissociation; (b) the product of Si−H dissociation; (c) the product of Si−C dissociation; (d) the transition state for C−H dissociation; (e) the transition state for Si−H dissociation; (f) the transition state for Si−C dissociation. Silicon atoms are in white; hydrogen atoms are in black; carbon atoms are in red.

with the carbon atom of the methylsilane molecule relatively close to the "down" silicon atom of the dimer with the formation of $Si-CH_2SiH_3$ and Si−H surface species. The transition state is located at 26.4 kcal/mol above the vacuum level, and the overall dissociative adsorption process is found to be 62.5 kcal/mol exothermic. On the Si(100)-2 × 1 surface, the Si−C dissociation is similar to C−H dissociation. The energy barrier is 35.0 kcal/mol, and the exothermicity of the overall dissociative adsorption process is 66.0 kcal/mol. The reaction pathway of Si−H dissociation is also a direct process by overcoming an energy barrier of 9.0 kcal/mol, resulting in the $Si-SiH_2CH_3$ and Si−H surface species. The exothermicity of the whole hydrogen dissociative adsorption process is 64.3 kcal/mol. This process is different from C−H and Si−C dissociation, initiated by the interaction of one hydrogen atom which attaches to the silicon atom in methylsilane molecule with the "down" (electrophilic) surface silicon atom. It is not a surprise that the electrophilic surface sites prefer to react with methylsilane by attacking one of the hydrogen atoms that belong to the silicon atom of methylsilane molecule since the hydrogen is more electronegative than silicon. The hydrogen atom is closer to the surface "down" silicon atom than to the silicon atom in methylsilane molecule in the transition state. The structure of the transition state indicates that the Si−H bond of methylsilane molecule is broken and a surface Si−H is being formed in the transition state. In the transition state, the distances between silicon atom of methylsilane molecule and the surface dimer silicon atoms ("down" and "up") are 2.586 and 3.115 Å, respectively, but both distances are too large for any significant bonding interaction. This is consistent with only a weak interaction between the $-SiH_2CH_3$ fragment and the nucleophilic surface silicon atom in the transition state. It can form a Si−Si bond to the nucleophilic surface silicon atom after the transition state is crossed, and our IRC calculations have confirmed it.

The reaction mechanism between methylsilane molecule and the Si(100)-2 × 1 surface is different from that of organic molecules containing oxygen atom and nitrogen atom on the Si(100)-2 × 1 surface. This may be attributed to no lone electron pair existing in the methylsilane molecule. Our calculations do not find evidence of any transition state characterized by a pentacoordinated silicon atom, as proposed by Xu et al.[5] To further check our calculations, we place a methylsilane molecule in such a way that its silicon atom is close to the "up" silicon atom (Si_{up}) of the surface dimer. Then we optimized the structure by fixing the $Si-Si_{up}$ bond at several distances (Figure 5). The total energy of the system monotonically increases by decreasing the $Si-Si_{up}$ distance, without any signature of the presence of a local minimum in the energy. The tendency of energies indicates that the pentacoordinated transition state does not exist. Similar results was obtained by Brown et al.,[49] who studied dissociative adsorption of SiH_4 on the Si(100) surface, and by Silverstreli et al.,[45] who also studied methylsilane on the Si-(100)-2 × 1 surface by the Car-Parrinello approach involving a periodically repeated slab of five Si layers and a vacuum region of 10 Å.

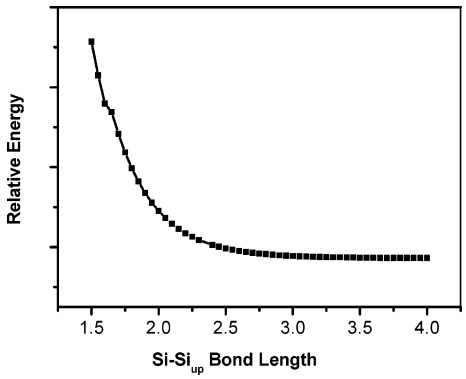

Figure 5. Energy profile by scanning different $Si-Si_{up}$ bond lengths under B3LYP/6-31G(d) level of theory. Bond length is in angstroms.

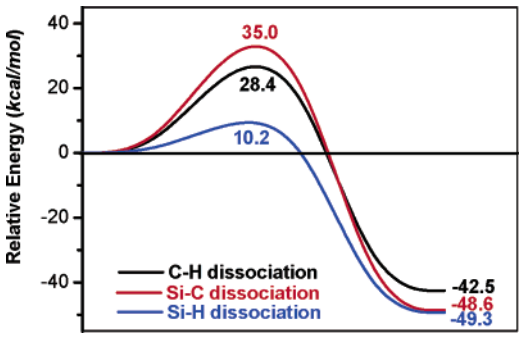

Figure 6. Reaction pathways for C−H, Si−C, and Si−H dissociation involving one dimer using $Si_{15}H_{16}$ cluster. The black curve represents the C−H dissociation; the red curve represents the Si−C dissociation; the blue curve represents the Si−H dissociation.

C. Dissociative Pathways of Methylsilane on One Dimer Involving a $Si_{15}H_{16}$ Two-Dimer Cluster. In this work, we also have calculated the dissociative reactions of methylsilane on one dimer involving a larger $Si_{15}H_{16}$ two-dimer cluster in order to study the cluster size effects on the activation energies of the surface reactions. The reaction pathways are shown in Figure 6, and the calculated transition states and dissociated states are presented in Figure 7. Our calculations indicate that the discrepancy of activation energies of three dissociative pathways using two different cluster models is less than 2 kcal/mol. Our calculated results using the $Si_{15}H_{16}$ cluster model have shown that the calculated results using the Si_9H_{12} cluster model lead to more than 15 kcal/mol difference in adsorption energies. However, when two calculated results involving Si_9H_{12} and $Si_{15}H_{16}$ cluster models are compared, the qualitative aspects of the potential energy surface remain the same.

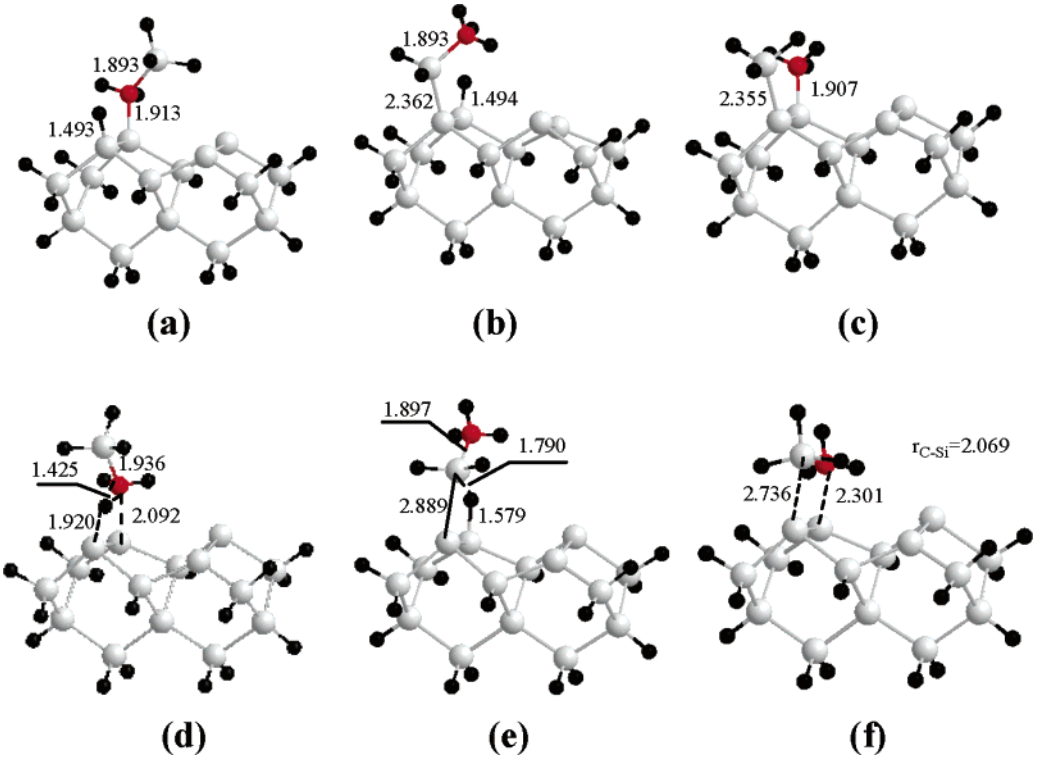

Figure 7. Calculated geometry structures of surface products and transition states along the surface reaction pathways involving one dimer using $Si_{15}H_{16}$ cluster: (a) the product of C−H dissociation; (b) the product of Si−H dissociation; (c) the product of Si−C dissociation; (d) the transition state for C−H dissociation; (e) the transition state for Si−H dissociation; (f) the transition state for Si−C dissociation. Silicon atoms are in white; hydrogen atoms are in black; carbon atoms are in red.

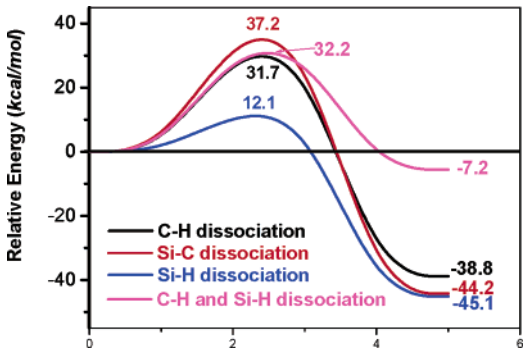

Figure 8. Reaction pathways for C−H, Si−C, and Si−H dissociation involving two adjacent dimers using $Si_{15}H_{16}$ two-dimer cluster. The black curve represents the C−H dissociation; the red curve represents the Si−C dissociation; the blue curve represents the Si−H dissociation; the magenta curve represents the dissociation of C−H and Si−H at the same time.

D. Dissociative Pathways of Methylsilane across Two Adjacent Dimers Using $Si_{15}H_{16}$ Cluster. The dissociative reactions also possibly occur across adjacent dimers along a dimer row. The calculated reaction pathways and the geometric structures of critical points are described in Figures 8 and 9, respectively. The energy barriers for C−H, Si−H, and Si−C dissociation are 31.7, 12.1, and 37.2 kcal/mol, respectively. The Si−H bond dissociation is the most kinetically favorable among three different dissociative reactions, similar to the calculated results involving one dimer using Si_9H_{12} and $Si_{15}H_{16}$ cluster models. When the calculated reaction pathways involving one dimer are compared, the calculated activation energies for three dissociative pathways at two adjacent dimers along a dimer row are higher. The interdimer distance between adjacent Si−Si dimers is 4.022 Å, much longer than the Si−Si bond length (2.225 Å) in a one-dimer cluster. The C−H bond is the shortest, and the increased activation energy is the largest. Therefore, such a larger interdimer distance may be unfavorable for C−H, Si−H, and Si−C dissociations. The calculated results using Si_9H_{12} and $Si_{15}H_{16}$ cluster models are summarized in Table 2. The decomposed products involving two adjacent dimers cause the rearrangement of surface silicon atoms. One of the silicon atoms of surface dimers transfers to a tetracoordinated atom by forming a new bond with the third-layer silicon atom and breaking a bond between one of the second-layer silicon atoms and the third-layer atoms as shown in Figure 9.

For the cross-dimer surface reactions, it is also possible that C−H and Si−H bonds dissociate at the same time. Our calculations capture a six-membered-ring transition state for this surface reaction as shown in Figure 9h. Such a reaction is a concentrated one. The free methylsilane molecule and bare surface overcome an activation energy of 32.2 kcal/mol, leading to the adsorption of two hydrogen atoms on the surface dimer and the formation of a free $CH_2{=}SiH_2$ molecule. The six-membered-ring transition state lowers the strain of the transition state and decreases the activation energy, compared with the total activation energies of the C−H dissociation and Si−H dissociation. However, the activation energy of C−H and Si−H dissociation at the same time is much higher than that of Si−H dissociation by 10.1 kcal/mol and the product is less stable than that of Si−H dissociation. Therefore, the formation of such a six-membered-ring transition state is unfavorable.

E. Competition of the Three Dissociative Pathways on the Si(100)-2 × 1 Surface. For free methylsilane molecule, the dissociation energies of C−H bond, Si−H bond, and Si−C bond are 99, 90, and 88 kcal/mol, respectively.[6] From a kinetic point of view, our calculated activation energy for Si−H bond cleavage is significantly the lowest, according to the above calculated results. Our calculated energy barriers and other theoretical results on silane[46,50] and chlorosilanes[28] for Si−H

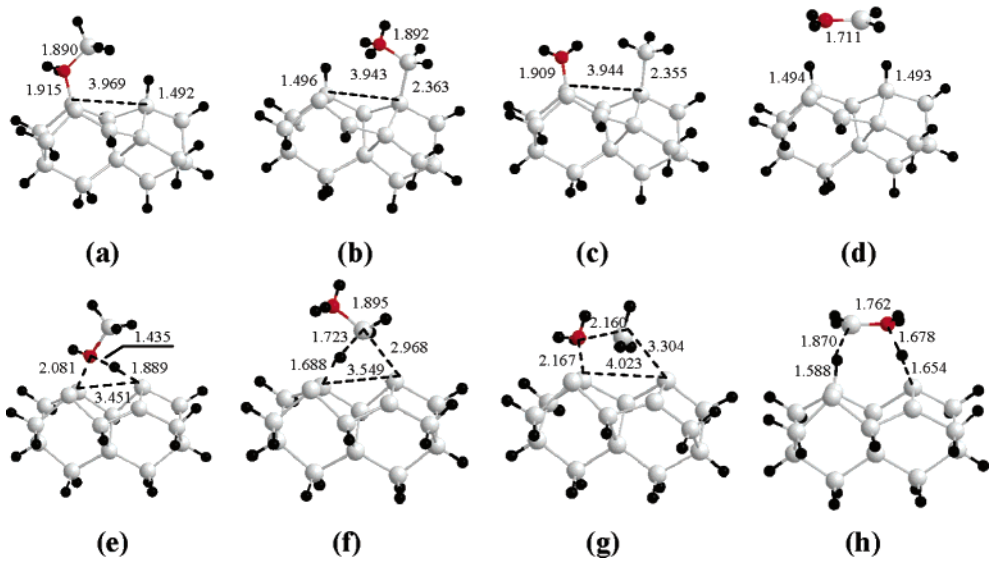

Figure 9. Calculated geometry structures of surface products and transition states along the surface reaction pathways involving two adjacent dimers using $Si_{15}H_{16}$ cluster: (a) the product of C−H dissociation; (b) the product of Si−H dissociation; (c) the product of Si−C dissociation; (d) the product of the dissociation of C−H and Si−H at the same time; (e) the transition state for C−H dissociation; (f) the transition state for Si−H dissociation; (g) the transition state for Si−C dissociation; (h) the six-membered-ring transition state for the dissociation of C−H and Si−H at the same time. Silicon atoms are in white; hydrogen atoms are in black; carbon atoms are in red.

TABLE 2: Summary of Calculated Results for One-Dimer and Two-Dimer Cluster Models[a]

	one-dimer		two-dimer		cross-dimer	
	E_a	E_{ad}	E_a	E_{ad}	E_a	E_{ad}
C−H dissociation	26.4	62.5	28.4	42.5	31.7	38.8
Si−H dissociation	9.0	64.3	10.2	49.3	12.1	45.1
Si−C dissociation	35.0	66.0	35.0	48.6	37.2	44.2

[a] E_a represents the activation energies, E_{ad} represents the adsorption energies of dissociation products, and all energies are in kcal/mol.

TABLE 3: Activation Energies for Different Silane Adsorptions via Si−H Dissociation

adsorption molecules	energy barrier (kcal/mol)
CH_3SiH_3	9.0[a]
CH_3SiH_3[46]	19.0
SiH_4[28,50]	11.3
SiH_3Cl[28]	4.5
SiH_2Cl_2[28]	10.5
$SiHCl_3$[28]	17.0
SiH_4[49]	12.0

[a] Si_9H_{12} cluster, this work.

dissociation are summarized in Table 3. Although our calculated activation barrier is lower than the value of Silvestrelli et al. by 10.0 kcal/mol, both calculations indicate that the Si−H dissociation is the most kinetically favorable at the Si(100)-2 × 1 surface. Comparing the structure at the transition states can highlight the differences in bond cleavage of free methylsilane and surface adsorption.

For C−H dissociation, this process is associated with the displacement of electron density from the carbon atom of the methylsilane molecule to the "down" silicon of the surface dimer. It is clear that this displacement will destroy the sp^3 hybridization of the carbon atom. It means that the three hydrogen atoms around the carbon atom have to spread in order to favor the "down" silicon to attract the electron from the carbon atom and one of the hydrogen atoms will transfer to the "up" silicon to keep sp^3 hybidization. This process needs extra energy to overcome the distortion of electron density. The case of Si−C dissociation is similar to that of C−H dissociation. The spatial structure and the electron density of carbon in the transition state have to distort to accommodate the electrophilic attack from the "down" surface silicon atom to the carbon atom. The energy barrier in this case is higher than C−H dissociation because the steric hindrance of the $-SiH_3$ group is much greater than that of the −H group. In the lowest energy barrier pathway of Si−H dissociation, the hydrogen atom being abstracted from methylsilane is forming a bond to the "down" surface silicon atom in the transition state. The Si−H bond-breaking process in methylsilane molecule is facilitated by electron donation from the "up" surface silicon. Compared to C−H and Si−C bond dissociation, little steric hindrance and no electron distortion exist in the transition state and the process of the leaving group ($-SiH_2CH_3$) transfer to the "up" surface silicon has little steric hindrance. As a result, the energy of the transition state is reduced and hence the Si−H dissociation process has a relatively low activation barrier. The same explanation can serve the dissociative reactions on two adjacent dimers along a dimer row.

Additional insight can be gained from examining the Si−H stretching modes of the reaction products. In Lee and Bent's work,[6] a strong and broad peak in the IR spectrum is centered around 2100 cm^{-1}. The author assigned this peak to a mix of silicon mono-, di-, and trihydride groups. The IR results show the SiC films contain primarily intact methyl groups and a range of SiH_x species, suggesting that the surface adsorbed species were formed mainly by the cleavage of the Si−H bond. Shinohara et al.[9,10] studied the Si−H stretching vibration region of the Si(100)-2 × 1 surface exposed to methylsilane by IRAS spectra at room temperature. An intense peak at 2080 cm^{-1} is attributed to monohydride, which is populated via the breaking of one of the three Si−H bonds of methylsilane molecule and the subsequent hydrogen termination of the dimer dangling bond. The IRAS spectra also indicates that the adsorption process also produces dihydride species $-SiH_2CH_3$ around 2120 cm^{-1}. Our results are consistent with the experimental results, 2096 and 2111 cm^{-1} (with a scale factor 0.9613 for frequencies), respectively, for monohydride species (Si−H) and dihydride species ($-SiH_2CH_3$), confirming the experimental data.

F. Stability of Dissociated Products. Since the growth temperature of SiC films by the CVD method using methylsilane

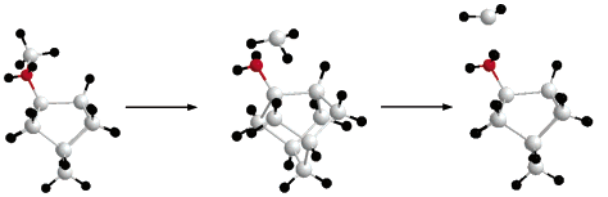

Figure 10. Reaction pathway for the direct desorption of SiH_2 from the $Si-CH_2SiH_3$ structure: (a) the $Si-CH_2SiH_3$ structure; (b) the transition state for the direct desorption of SiH_2; (c) the desorption product.

as source is high, it is possible that the direct desorption of SiH_x and CH_x occurs from dissociated products. If direct desorption occurs, the Si:C = 1 ratio of SiC films cannot be preserved, resulting in imperfect films. However, most applications require production of SiC films with a Si:C ratio of exactly 1:1. Therefore, it is necessary to examine the stability of dissociated products. We have calculated the pathways of direct desorption of SiH_2 and CH_2 from the dissociated products $Si-CH_2SiH_3$ and $Si-SiH_2CH_3$. According to the above analysis, cluster size effects have little influence on the activation energies. We carry out our calculations using Si_9H_{12} cluster to minimize computational cost. The calculated energy barrier for the desorption of SiH_2 from $Si-CH_2SiH_3$ structure is 86.9 kcal/mol by using the Si_9H_{12} cluster model, and the optimized structures along the potential energy surface are shown in Figure 10. However, we did not locate the transition state for the direct desorption of CH_2 from the $Si-SiH_2CH_3$ structure. Lee and Bent's work[6] has suggested that the methyl groups are more stable than SiH_3 groups and that they do not decompose to CH_2 at high temperature. Therefore, we believe that the direct desorption of CH_2 is more difficult from the $Si-SiH_2CH_3$ structure. The results of both experiments and theoretical calculations have proved that the Si−H dissociation is the main surface reaction at the low temperature. Therefore, the majority of Si−C bonds can be kept intact during the CVD process.

4. Conclusion

In this work, we have studied the surface dissociative reactions of methylsilane on the Si(100)-2 × 1 surface during the initial steps of surface adsorption by density functional theory. Our calculations show that no preadsorbed states of nondissociative methylsilane molecule exist before Si−H, C−H, and Si−C bond dissociation. Our calculated results indicate that the Si−H dissociation is kinetically favorable over C−H and Si−C bond dissociation not only on the one-dimer cluster but also on the two-dimer cluster. The dissociative reactions across two adjacent dimers along a dimer row lead to rearrangement of silicon atoms. A structural interpretation of the transition states is presented to account for the selectivity of different dissociative pathways. Finally, we analyze the stability of dissociated products by DFT calculations and show that methylsilane should be a good candidate for the growth of SiC films.

Acknowledgment. This work was supported by NKBRSF (1999075302), the Knowledge Innovation Program of the Chinese Academy of Sciences (Grant DICP K2001/E3), and NSFC. We also express our gratitude to Mr. Wang Yong for his stimulating interest in our theoretical results and his useful comments.

References and Notes

(1) Addamiano, A.; Klein, P. H. *J. Cryst. Growth* **1984**, *70*, 291.
(2) Shibahara, K.; Nishino, S.; Matsunami, H. *J. Cryst. Growth* **1986**, *78*, 538.
(3) Reidinger, F. G.; Marti, J. *Appl. Phys. Lett.* **1992**, *60*, 1703.
(4) Johnson, A. D.; Perrin, J.; Mucha, J. A.; Ibbotson, D. E. *J. Phys. Chem.* **1993**, *97*, 12937.
(5) Xu, J.; Choyke, W. J.; Yates, J. T., Jr. *J. Phys. Chem. B* **1997**, *101*, 6879.
(6) Lee, M. S.; Bent, S. F. *J. Phys. Chem. B* **1997**, *101*, 9195.
(7) Yasui, K.; Asada, K.; Maeda, T.; Akahane, T. *Appl. Surf. Sci.* **2001**, *175−176*, 495.
(8) Takatsuka, T.; Fujiu, M.; Sakuraba, M.; Matsuura, T.; Murota, J. *Appl. Surf. Sci.* **2000**, *162−163*, 156.
(9) Shinohara, M.; Maehama, T.; Niwano, M. *Appl. Surf. Sci.* **2000**, *162−163*, 161.
(10) Shinohara, M.; Kimura, Y.; Shoji, D.; Niwano, M. *Appl. Surf. Sci.* **2001**, *175−176*, 591.
(11) Kim, K. C.; Nahm, K. S.; Hahn, Y. B.; Lee, Y. S.; Byun, H. S. *J. Vac. Sci. Technol., A* **2000**, *18*, 891.
(12) Boo, J.; Ustin, S. A.; Ho, W. *Thin Solid Films* **1999**, *343−344*, 650.
(13) Takahashi, K.; Nishino, S.; Saraie, J. *J. Electrochem. Soc.* **1992**, *139*, 3565.
(14) Chiu, H. T.; Hsu, J. S. *Thin Solid Films* **1994**, *252*, 13.
(15) Yuan, C.; Steckl, A. J.; Loboda, M. J. *Appl. Phys. Lett.* **1994**, *64*, 3000.
(16) Lee, K. W.; Yu, K. S.; Kim, Y. *J. Cryst. Growth* **1997**, *179*, 153.
(17) Boo, J. H.; Yu, K. S.; Lee, M.; Kim, Y. *Appl. Phys. Lett.* **1995**, *66*, 3486.
(18) Mui, C.; Bent, S. F.; Musgrave, C. B. *J. Phys. Chem. A* **2000**, *104*, 2457.
(19) Barriocanal, J. A.; Doren, D. J. *J. Vac. Sci. Technol., A* **2000**, *18*, 1959.
(20) Barriocanal, J. A.; Doren, D. J. *J. Phys. Chem. B* **2000**, *104*, 12269.
(21) Widjaja, Y.; Mysinger, M. M.; Musgrave, C. B. *J. Phys. Chem. B* **2000**, *104*, 2527.
(22) Widjaja, Y.; Musgrave, C. B. *Surf. Sci.* **2000**, *469*, 9.
(23) Lu, X.; Zhang, Q.; Lin, M. C. *Phys. Chem. Chem. Phys.* **2001**, *3*, 2156.
(24) Wang, G. T.; Mui, C.; Musgrave, C. B.; Bent, S. F. *J. Phys. Chem. B* **2001**, *105*, 3295.
(25) Lu, X.; Xu, X.; Wang, N. Q.; Zhang, Q.; Lin, M. C. *J. Phys. Chem. B* **2001**, *105*, 10069.
(26) Kato, T.; Kang, S. Y.; Xu. X.; Yamabe, T. *J. Phys. Chem. B* **2001**, *105*, 10340.
(27) Gladden, F. B.; Lu, X.; Lin, M. C. *J. Phys. Chem. B* **2001**, *105*, 4368.
(28) Hall, M. A.; Mui, C.; Musgrave, C. B. *J. Phys. Chem. B* **2001**, *105*, 12068.
(29) Barriocanal, J. A.; Doren, D. J. *J. Am. Chem. Soc.* **2001**, *123*, 7340.
(30) Widjaja, Y.; Musgrave, C. B. *J. Chem. Phys.* **2002**, *116*, 5774.
(31) Widjaja, Y.; Heyman, A.; Musgrave, C. B. *J. Phys. Chem. B* **2002**, *106*, 2643.
(32) Wang, G. T.; Mui, C.; Musgrave, C. B.; Bent, S. F. *J. Am. Chem. Soc.* **2002**, *114*, 8990.
(33) Lu, X. *J. Am. Chem. Soc.* **2003**, *125*, 6384.
(34) Wang, G. T.; Mui, C.; Tannaci, J. F.; Filler, M. A.; Musgrave, C. B. *J. Phys. Chem. B* **2003**, *107*, 4982.
(35) Widjaja, Y.; Han, J. H.; Musgrave, C. B. *J. Phys. Chem. B* **2003**, *107*, 9319.
(36) Mui, C.; Filler, M. A.; Bent, S. F.; Musgrave, C. B. *J. Phys. Chem. B* **2003**, *107*, 12256.
(37) Widjaja, Y.; Musgrave, C. B. *Surf. Sci.* **2000**, *469*, 9.
(38) Becke, A. D. *J. Chem. Phys.* **1993**, *98*, 1372.
(39) Becke, A. D. *J. Chem. Phys.* **1993**, *98*, 5648.
(40) Lee, C.; Yang, W.; Parr, R. G. *Phys. Rev. B* **1988**, *37*, 785.
(41) Hohenberg, P.; Kohn, W. *Phys. Rev.* **1964**, *136*, B864−B871.
(42) Kohn, W.; Sham, L. J. *Phys. Rev.* **1965**, *140*, A1133−A1138.
(43) Frisch, M. J.; Trucks, G. W.; Schlegel, H. B.; Scuseria, G. E.; Robb, M. A.; Cheeseman, J. R.; Zakrzewski, V. G.; Montgomery, J. A., Jr.; Stratmann, R. E.; Burant, J. C.; Dapprich, S.; Millam, J. M.; Daniels, A. D.; Kudin, K. N.; Strain, M.; Pomelli, C.; Adamo, C.; Clifford, S.; Ochterski, J.; Petersson, G. A.; Ayala, P. Y.; Cui, Q.; Morokuma, K.; Malick, D. K.; Rabuck, A. D.; Raghavachari, K.; Foresman, J. B.; Cioslowski, J.; Oritz, J. V.; Stefanov, B. B.; Liu, G.; Liashenko, A.; Piskorz, P.; Komaromi, I.; Gomperts, R.; Martin, R. L.; Fox, D. J.; Keith, T.; Al-Laham, M. A.; Peng, C. Y.; Nanayakkara, A.; Gonzalez, C.; Challacombe, M.; Gill, P. M. W.; Johnson, B. G.; Chen, W.; Wong, M. W.; Andres, J. L.; Head-Gordon, M.; Replogle, E. S.; Pople, J. A. *Gaussian 98*; Gaussian Inc.: Pittsburgh, PA, 1998.
(44) Duncan, J. L.; Harvie, J. L.; Mckean, D. C. *J. Mol. Struct.* **1986**, *145*, 225.

(45) Shimanouchi, T. *Tables of Molecular Vibrational Frequencies Consolidated*; National Bureau of Standards: Washington, DC, 1972; Vol. 1.
(46) Silverstreli, P. L.; Sbraccia, C.; Ancilotto, F. *J. Chem. Phys.* **2002**, *116*, 6291.
(47) Komornicki, T. *J. Am. Chem. Soc.* **1984**, *106*, 3114.
(48) Breneman, C. M.; Wiberg, K. B. *J. Comput. Chem.* **1990**, *11*, 361.
(49) Brown, A. R.; Doren, D. J. *J. Chem. Phys.* **1999**, *110*, 2643.
(50) Kang, J. K.; Musgrave, C. B. *Phys. Rev. B* **2001**, *64*, 245330.